UDC 621.039.51

Badawi M.S.[a], El-Khatib A.M.[a], Elzaher M.A.[b], Thabet A.A.[c] , Sakr A.A.[d]

[a] Physics Department, Faculty of Science, Alexandria University, 21511 Alexandria, Egypt.

[b] Department of Basic and Applied Sciences, Faculty of Engineering, Arab Academy for Science, Technology and Maritime Transport, Alexandria, Egypt.

[c] Department of Medical Equipment Technology, Pharos University in Alexandria, Egypt

[d] Physics Department, Faculty of Science, Damanhour University, Egypt.

USING AN ANALYTICAL EFFICIENCY TRANSFER PRINCIPLE TO CALCULATE THE FULL ENERGY PEAK EFFICIENCY FOR GAMMA DETECTORS

In this work the Full-Energy Peak Efficiency of NaI(Tl) - scintillation detectors (5.08x5.08 cm²and 7.62x7.62 cm²) values have been calculated for axial cylindrical sources of different dimensions larger than the detectors using an analytical approach of effective solid angle calculation. This approach is based on the ratio of the source-detector solid angle with taken the source self absorption effect in to account. The detector efficiency for various geometrical conditions is derived from the known efficiency for reference source-detector geometry. The present method shows a great possibilities to calibrate the detectors through the determination of the full-energy peak efficiency curve even in those case when no standard source is available and this consider as the final goal of this work.

Keywords: NaI (Tl) detector, Full-Energy Peak Efficiency, Efficiency Transfer.

1. Introduction

In gamma-ray spectroscopy, one usually needs to know the full-energy peak efficiency for any specific source–detector configuration of concern. Because the experimental work isis an inflexible and a time consuming process, much research have been focused on the development of computational techniques to determine different efficiencies. One of these techniques is the efficiency transfer principle in which the computation of the detector efficiency for various geometrical conditions is derived from the known efficiency for reference source-detector geometry. The efficiency transfer method is particularly useful due to its insensitivity to the inaccuracy of the input data, such as the uncertainty of the detector characterization (Le`py et al., [1]; Vidmar et al. [2]). The presented approach is based on the direct mathematical method reported by Selim and Abbas [3–10], which used successfully before to calibrate different sources with different detectors.

2. Mathematical treatment

Selim and Abbas used the spherical coordinate system to derive the direct analytical elliptic integrals and to calculate different detector efficiencies for any source-detector configuration. The solid angle (Ω) subtended by the detector at the source point is introduced in Abbas [7], and it is defined as:

$$\Omega = \int_{\theta}\int_{\varphi} \sin\theta \, d\varphi d\theta \, . \qquad (4)$$

So the effective solid angle can be defined as:

$$\Omega_{eff} = \int_{\theta}\int_{\varphi} f_{att} . \sin\theta d\varphi d\theta \, . \qquad (5)$$

where f_{att} is the factor that determines the photon attenuation by all absorbers between source and detector, it is expressed as:

$$f_{att} = e^{-\sum_i \mu_i \delta_i} \qquad (6)$$

where μ_i is the attenuation coefficient of the i^{th} absorber for a gamma-ray photon with energy E_γ and δ_i is the average gamma photon path length through the i^{th} absorber.

In the case of an axial point source at distance (h) from the detector as shown in figure (1), it makes polar (θ) and the azimuth (φ) angles which are at the point of entrance of the considered surface defined by the direction of the incidence of a gamma-ray photon.

The polar angles can be expressed as, Abbas [7]

$$\theta_1 = \tan^{-1}\left(\frac{R}{h+L}\right) \;\&\; \theta_2 = \tan^{-1}\left(\frac{R}{h}\right). \qquad (7)$$

Therefore the effective solid angle can be expressed as:

$$\Omega_{eff} = \int_0^{\theta_1}\int_0^{2\pi} f_{att} \sin\theta d\varphi \, d\theta \; + \; \int_{\theta_1}^{\theta_2}\int_0^{2\pi} f_{att} \sin\theta d\varphi \, d\theta \, . \qquad (8)$$

Volumetric source can be treated as group of point sources which are uniformly distributed; each

point source has an effective solid angle $\Omega_{eff\,(Point)}$ Nafee [11] as shown in equation (9).

$$\Omega_{eff\,(Cyl)} = \frac{\int_{v} f_{att} \cdot \Omega_{eff\,(Point)}\, dV}{V} . \qquad (10)$$

For an arbitrary element of volume dV at lateral distance ρ from the detector axis that makes an angle α with the detector's major axis h. Where h is the source-detector separation, this element of volume can be expressed in the polar coordinates by:

$$dV = \rho d\rho d\alpha dh .$$

Therefore, equation (9) will be:

$$\Omega_{eff\,(Cyl)} = \frac{\int_{h}\int_{\alpha}\int_{\rho} f_{att} \cdot \Omega_{eff\,(Point)} \cdot \rho d\rho d\alpha dh}{V} . \qquad (11)$$

In volumetric source, not all the emitted photons from the source exit from it, but part of them is absorbed in the source itself, which affects the effective solid angle calculations. The factor concerning this effect is called the self-absorption factor S_f which is given by: [11]

$$S_f = e^{-\mu_s . d_s} \qquad (12)$$

where μ_s is the source attenuation coefficient and d_s is the distance traveled by the emitted photon inside the source as shown in figure (2). d_s was found to be a function of the polar and azimuthal angles (θ, φ) inside the source itself and it is given by:

$$d_{s_1} = \frac{h - h_o}{\cos\theta} \quad for\ \theta \le \theta_2^{'} \quad and \quad \varphi \le \varphi_{S\max}^{'} . \qquad (13)$$

Therefore, the source polar and azimuthal angles can be given as equations (14) and (15), respectively: [11]

$$\theta_1^{'} = \tan^{-1}\left(\frac{S-\rho}{h-h_o}\right) \quad \& \quad \theta_2^{'} = \tan^{-1}\left(\frac{S+\rho}{h-h_o}\right) \qquad (14)$$

$$\varphi_{S\max}^{'} = \cos^{-1}\left(\frac{\rho^2 - S^2 + (h-h_o)^2 \tan^2}{2\rho(h-h_o)\tan}\right) . \qquad (15)$$

Where θ'_1 and θ'_2 are the extreme polar angles of the source, $\varphi'_{S\max}$ is the maximum azimuthal angle for the photon to exit the source, and ho is the source-detector separation.

So equation (11) can be written as follows:

$$\Omega_{eff\,(Cyl)} = \frac{\int_{h}\int_{\alpha}\int_{\rho} f_{att} \cdot S_f \cdot \Omega_{eff\,(Point)} \cdot \rho d\rho d\alpha dh}{V} . \qquad (16)$$

Thus, the effective solid angle of a cylindrical detector in case of a cylindrical source of radius (S≥R) and height H can be expressed by:

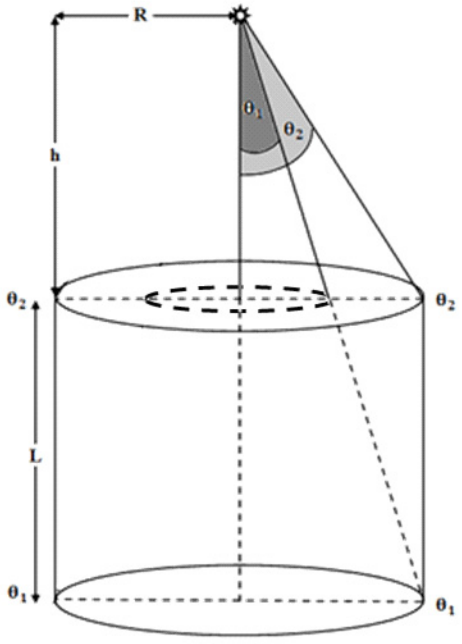

Figure 1 The axial point source with Cylindrical Detector

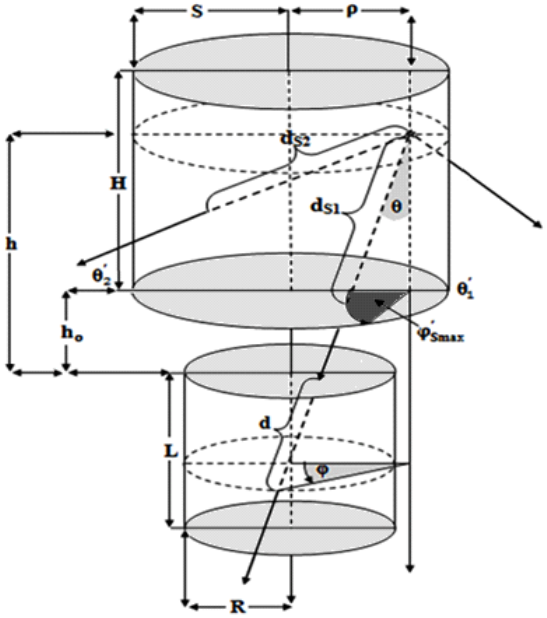

Figure 2 Cylindrical source and detector configuration (S≥R)

$$\Omega_{eff\,(Cyl)} = \frac{\int_{h_o}^{H+h_o}\int_{0}^{2\pi}\int_{0}^{S} f_{att}.\,S_f.\Omega_{eff\,(Po\,\mathrm{int})}.\rho d\rho d\alpha dh}{\pi\, S^2 H} .(17)$$

So the detector efficiency using cylindrical sources can be calculated by the efficiency transfer principle as follow:

$$\varepsilon\left(E,Cyl\right)=\varepsilon\left(E,P_o\right)\frac{\Omega_{eff}\left(Cyl\right)}{\Omega_{eff}\left(P_o\right)}. \qquad (18)$$

3. Experimental setup

In this work two NaI (Tl) scintillation detectors are used. The (5,08x5,08 cm^2) detector (D1) and (7,62x7,62 cm^2) detector (D2) details are listed in table 1.

The FEPE has been measured using two types of radioactive sources. The point sources for first one are ^{241}Am, ^{133}Ba, ^{152}Eu, ^{137}Cs, and ^{60}Co. point sources were purchased from the Physikalisch-Technische Bundesanstalt (PTB) in Braunschweig and Berlin. The certificates show the sources activities and their uncertainties for PTB sources which are listed in table 2. The data sheet states the values of half-life photon energies and photon emission probabilities per decay for all radionuclides used in the calibration process are listed in table 3, which is available at the National Nuclear Data Center Web Page or on the IAEA website.

The calibration process was done by using the (PTB) point sources. Homemade Plexiglas holder is used to measure these sources at three different axial distances starting from 20, 25, and 30 cm from the detectors surface. The holder is placed directly on the detector entrance window as an absorber. In most cases the accompanying x-ray was soft enough to be absorbed completely before entering the detector. To avoid the effect of в- and x- rays and to protect the detector heads, therefore, there is no correction was made for x-gamma coincidences. The source-detector separations start from 20 cm to neglect the coincidence summing correction.

The second type of source is the 500 ml Polypropylene volumetric source made by Nalgene Lab-ware, its catalog number is (NG-2118), the size code is (16) filled with 200, 300, and 400 ml ^{152}Eu solution of known activity with heights 21.45 mm,

Table 1 Detectors setup parameters with acquisition electronics specifications for Detector (D1) and Detector (D2)

Items	Detector (D1)	Detector (D2)
Manufacturer	Canberra	Canberra
Serial Number	09L 654	09L 652
Detector Model	802	802
Type	cylindrical	cylindrical
Mounting	vertical	vertical
Resolution (FWHM) at 661 kev	7.5%	8.5%
Cathode to Anode voltage	+1100 V dc	+1100 V dc
Dynode to Dynode	+80 V dc	+80 V dc
Cathode to Dynode	+150 V dc	+150 V dc
Tube Base	Model 2007	Model 2007
Shaping Mode	Gaussian	Gaussian
Detector Type	NaI(Tl)	NaI(Tl)
Crystal Diameter (mm)	50.8	76.2
Crystal Length (mm)	50.8	76.2
Top cover Thickness(mm)	Al (0.5)	Al (0.5)
Side cover Thickness(mm)	Al (0.5)	Al (0.5)
Reflector – Oxide (mm)	2.5	2.5
Weight (Kg)	0.77	1.8
Outer Diameter(mm)	57.2	80.9
Outer Length(mm)	53.9	79.4
Crystal Volume in (cm^3)	103.004	347.639

Table 2 PTB point sources activities and their uncertainties

PTB-Nuclide	Activity (KBq)	Reference Date 00:00 Hr	Uncertainty (KBq)
^{241}Am	259.0	1.June 2009	2.6
^{133}Ba	275.3		2.8
^{152}Eu	290.0		4.0
^{137}Cs	385.0		4.0
^{60}Co	212.1		1.5

Table 3 Half lives, photon energies and photon emission probabilities per decay for the all radionuclides used in this work

PTB-Nuclide	Energy (Kev)	Emission Probability %	Half Life (Days)
^{241}Am	59.52	35.9	157861.05
^{133}Ba	80.99	34.1	3847.91
^{152}Eu	121.78	28.4	4943.29
	244.69	7.49	
	344.28	26.6	
	778.9	12.96	
	964.13	14.0	
	1408.01	20.87	
^{137}Cs	661.66	85.21	11004.98
^{60}Co	1173.23	99.9	1925.31
	1332.5	99.982	

31.59 mm and 41.83 mm respectively, the details of the prepared sources are tabulated in table (4)

As an example if the spectrum was recorded as P4D1 where P refers to the source type (point) measured on detector (D1) at distance number (4), hence h = 20 cm.

The volumetric sources (vials) were measured on a 0.1 cm thick Plexiglas cover and placed directly on the detector end-cap. These measurements were done using two cylindrical detectors with numbers (D1 and D2). The source was placed on the detector end-cap with the center of the source centered on the end-cap. The spectra was recorded as V1D2, where V1 is the volume (V1) measured on detector (D2). The angular correlation effects can be neglected for the low source-to-detector distance, Debertin, et al., [12]

The spectrum acquired with winTMCA32 software is made by ICx Technologies. It was analyzed with Genie 2000 data acquisition and analysis software. It was made by Canberra using the automatic peak search and the peak area calculations, along with changes in the peak fit using the interactive peak fit interface when necessary to reduce the residuals and errors in the peak area values. The live time, the run time, and the start time for each spectrum are entered in the spread sheets. Those sheets were used to perform the calculations necessary to generate the experimental FEPE curves with their associated uncertainties as a function of the photon energy for all calibration sources detectors listed in tables (4).

The Efficiency Transfer Theoretical Method (ETTM) used to convert the FEPE curve from point sources at position (P4, P5, P6) to the FEPE of other geometries which represented in V1, V2, and V3. These calculations extended for two cylindrical NaI(Tl) detectors (D1, and D2).

4. Results and Discussions

This section shows a comparison between the theoretical and the experimental work of the efficiency transfer method (ETTM). The experimental work was held at Younis. S. Selim laboratory for Radiation Physics, Faculty of Science, Alexandria University. This laboratory uses several coaxial NaI (Tl) scintillation detectors (5.08x5.08 cm^2 and 7.62x7.62 cm^2) which are used in the presented work. The detectors were calibrated by measuring the low activity point sources, previously described. The theoretical FEPE can be obtained as given in equation (18).

The percentage error between the measured and the calculated efficiencies is given by:

$$\Delta\% = \frac{\varepsilon_{ETTM} - \varepsilon_{meas}}{\varepsilon_{meas}} \times 100 \qquad (19)$$

where ε_{cal} and ε_{meas} are the calculated and experimentally measured efficiencies, respectively.

The measured efficiency values as a function of the photon energy $\varepsilon(E)$ for all NaI Scintillation detectors were calculated by:

$$\varepsilon(E) = \frac{N(E)}{T \cdot A_S \cdot P(E)} \prod C_i \qquad (20)$$

where $N(E)$ is the number of counts in the full-energy peak and it can be obtained using Genie 2000 software, T is the measuring time (in second), $P(E)$ is the photon emission probability at energy E, A_S is the radionuclide activity, and C_i, are the correction factors due to dead time and radionuclide decay.

For the measurements of the low activity sources, the dead time was always less than 3%, so the corresponding factor was obtained simply using ADC live time. The statistical uncertainties of the net peak areas were smaller than 1,0 %. Since the acquisition time was long enough to get the number of counts which was at least 10,000 counts. Therefore, the background subtraction was done. The decay correction C_d for the calibration source from the reference time to the run time was given by:

$$C_d = e^{\lambda \cdot \Delta T} \qquad (21)$$

where λ is the decay constant and ΔT is the time interval over which the source decays corresponding to the run time. The main source of uncertainty in the efficiency calculations was the uncertainties of the activities of the standard source solutions. The coincidence summing effects were negligible in the reference measurement geometries.

Table 4 Prepared sources (homemade) details

Volume	Nuclide	Activity (KBq)	Reference Date 00:00 Hr	Uncertainty (%)
V1 (200 ml)				
V2 (300 ml)	^{152}Eu	5	1.Jan 2010	1.98
V3(400 ml)				

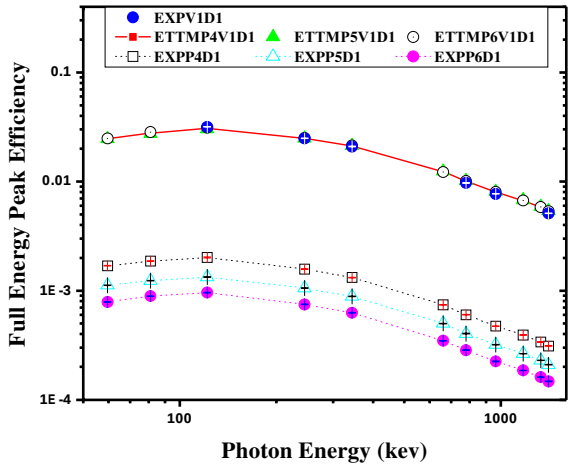

Figure 3 ETTM efficiency results for conversion from point sources at (P4, P5, and P6) to V1 using detector (D1), and the measured one for (V1D1) arrangement

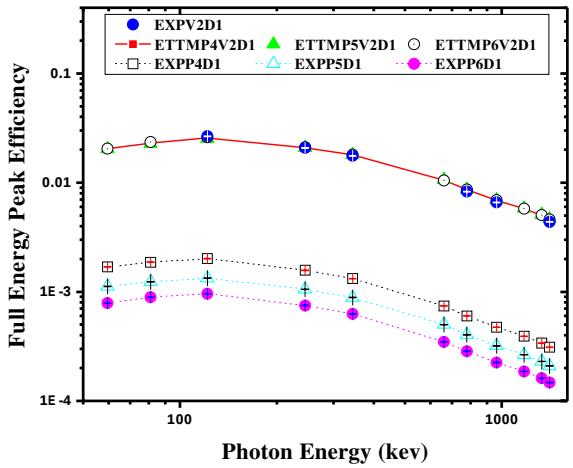

Figure 4 ETTM efficiency results for conversion from point sources at (P4, P5, and P6) to V2 using detector (D1), and the measured one for (V2D1) arrangement

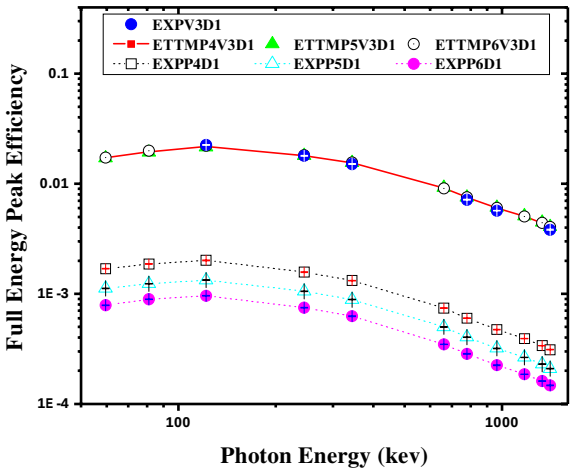

Figure 5 ETTM efficiency results for conversion from point sources at (P4, P5, and P6) to V3 using detector (D1), and the measured one for (V3D1) arrangement

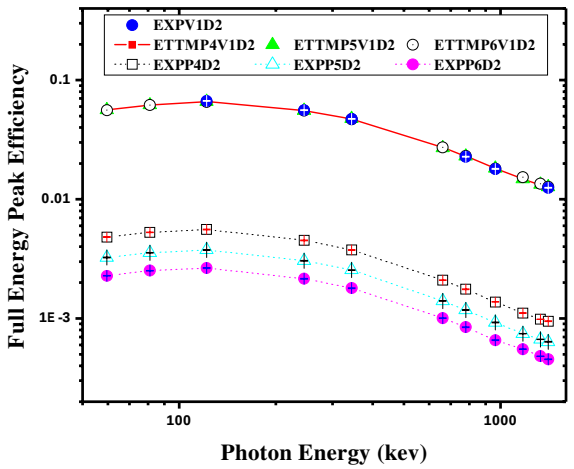

Figure 6 ETTM efficiency results for conversion from point sources at (P4, P5, and P6) to V1 using detector (D2), and the measured one for (V1D2) arrangement

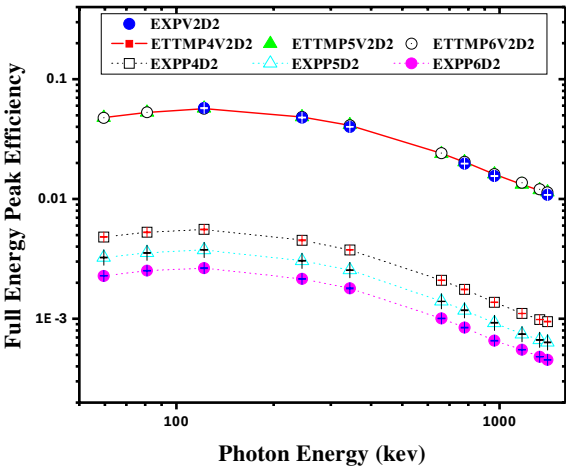

Figure 7 ETTM efficiency results for conversion from point sources at (P4, P5, and P6) to V2 using detector (D2), and the measured one for (V2D2) arrangement

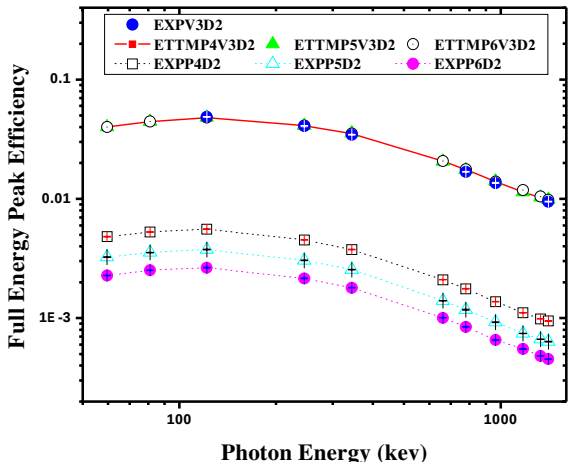

Figure 8 ETTM efficiency results for conversion from point sources at (P4, P5, and P6) to V3 using detector (D2), and the measured one for (V3D2) arrangement

The uncertainty in the FEPE σ_ε was given by:

$$\sigma_\varepsilon = \varepsilon \cdot \sqrt{\left(\frac{\partial \varepsilon}{\partial A}\right)^2 \cdot \sigma_A{}^2 + \left(\frac{\partial \varepsilon}{\partial P}\right)^2 \cdot \sigma_P{}^2 + \left(\frac{\partial \varepsilon}{\partial N}\right)^2 \cdot \sigma_N{}^2} \qquad (22)$$

where σ_A, σ_P, and σ_N, are the uncertainties associated with the quantities A_s, $P(E)$, and $N(E)$, respectively, assuming that the only correction made is due to the source activity decay.

In order to study the effect of the detector volume and the source-to-detector distance on the FEPE of NaI (Tl) detectors (D1 and D2) and of volumes (V1, V2, and V3), the measured efficiency for different sources detector arrangement were compared. Figure (3–8) show that the efficiency is increasing by decreasing the source volume (all sources have the same radius, vessel, and carrier solution, only the height of the source is different). The self-attenuation effect increased by increasing the carrier solution as we know when the attenuation factors increase then the number of photons

Table 5.a The Discrepancy percentage (Δ%) between the experimental and theoretical for (ETTM) values using detector D1 and volume sources V1,V2 and V3

Nuclide	Energy	V1D1	P4V1D1		P5 V1D1		P6 V1D1	
			ETTM	Δ%	ETTM	Δ%	ETTM	Δ%
Am-241	59.53		2.476E-02		2.453E-02		2.482E-02	
Ba-133	80.99		2.783E-02		2.747E-02		2.842E-02	
Eu-152	121.78	3.168E-02	3.064E-02	-3.262%	3.032E-02	-4.274%	3.116E-02	-1.641%
Eu-152	244.69	2.488E-02	2.486E-02	-0.102%	2.485E-02	-0.127%	2.506E-02	0.712%
Eu-152	344.28	2.090E-02	2.120E-02	1.451%	2.129E-02	1.895%	2.134E-02	2.124%
Cs-137	661.66		1.232E-02		1.242E-02		1.222E-02	
Eu-152	778.9	9.719E-03	1.008E-02	3.718%	1.012E-02	4.084%	1.008E-02	3.708%
Eu-152	964.13	7.710E-03	8.010E-03	3.895%	8.084E-03	4.847%	8.033E-03	4.197%
Co-60	1173.23		6.687E-03		6.755E-03		6.708E-03	
Co-60	1332.5		5.821E-03		5.890E-03		5.847E-03	
Eu-152	1408.01	5.118E-03	5.352E-03	4.558%	5.383E-03	5.178%	5.342E-03	4.369%
Nuclide	Energy	V2D1	P4V2D1		P5 V2D1		P6 V2D1	
			ETTM	Δ%	ETTM	Δ%	ETTM	Δ%
Am-241	59.53		2.044E-02		2.025E-02		2.049E-02	
Ba-133	80.99		2.310E-02		2.280E-02		2.358E-02	
Eu-152	121.78	2.663E-02	2.557E-02	-3.968%	2.530E-02	-4.973%	2.600E-02	-2.359%
Eu-152	244.69	2.083E-02	2.095E-02	0.604%	2.095E-02	0.579%	2.113E-02	1.424%
Eu-152	344.28	1.763E-02	1.797E-02	1.912%	1.805E-02	2.357%	1.809E-02	2.587%
Cs-137	661.66		1.055E-02		1.063E-02		1.045E-02	
Eu-152	778.9	8.270E-03	8.645E-03	4.534%	8.676E-03	4.902%	8.644E-03	4.523%
Eu-152	964.13	6.580E-03	6.889E-03	4.690%	6.952E-03	5.649%	6.909E-03	4.994%
Co-60	1173.23		5.766E-03		5.824E-03		5.784E-03	
Co-60	1332.5		5.027E-03		5.086E-03		5.049E-03	
Eu-152	1408.01	4.382E-03	4.625E-03	5.544%	4.652E-03	6.170%	4.616E-03	5.353%
Nuclide	Energy	V3D1	P4V3D1		P5 V3D1		P6 V3D1	
			ETTM	Δ%	ETTM	Δ%	ETTM	Δ%
Am-241	59.53		1.722E-02		1.705E-02		1.726E-02	
Ba-133	80.99		1.953E-02		1.928E-02		1.995E-02	
Eu-152	121.78	2.247E-02	2.173E-02	-3.285%	2.150E-02	-4.297%	2.209E-02	-1.665%
Eu-152	244.69	1.792E-02	1.796E-02	0.246%	1.796E-02	0.222%	1.811E-02	1.064%
Eu-152	344.28	1.514E-02	1.547E-02	2.173%	1.554E-02	2.619%	1.557E-02	2.850%
Cs-137	661.66		9.154E-03		9.228E-03		9.074E-03	
Eu-152	778.9	7.156E-03	7.519E-03	5.071%	7.545E-03	5.441%	7.518E-03	5.060%
Eu-152	964.13	5.688E-03	6.006E-03	5.598%	6.061E-03	6.565%	6.024E-03	5.904%
Co-60	1173.23		5.037E-03		5.089E-03		5.054E-03	
Co-60	1332.5		4.398E-03		4.450E-03		4.417E-03	
Eu-152	1408.01	3.819E-03	4.048E-03	5.996%	4.072E-03	6.625%	4.041E-03	5.805%

reach the detector decrease. Moreover, the efficiency is increased with increasing the detector's volume, where the crystal should be long enough to have reasonable efficiency for the highest energy gamma-rays of interest. This is due to the change in solid angle and increasing the chance of various interactions of photon with the detector material as a result of increasing the pass length in the crystal of larger volume.

The efficiency of the detectors is high at low source energies (absorption coefficient is very high) and decreases as the energy increases (fall off in the absorption coefficient). This is due to the fact that the photoelectric is dominant below 100 keV, which means in other words that it is higher for the bigger detector than the smaller one and it is higher for lower source energy than higher source energy. This is because of the dominance of the photoelectric at lower source energies.

The presented work provides a great understanding to several aspects of gamma-ray spectroscopy and will provide us with useful tools (ETTM) for efficiency calculation for co-axial detectors. This method constitutes a good approach for the efficiency computation for laboratory routine measurements and can save time in avoiding experimental

Table 5.b The Discrepancy percentage (Δ%) between the experimental and theoretical for (ETTM) values using detector D1 and volume sources V1, V2 and V3

Nuclide	Energy	V1D2	P4V1D2		P5 V1D2		P6 V1D2	
			ETTM	Δ%	ETTM	Δ%	ETTM	Δ%
Am-241	59.53		5.624E-02		5.619E-02		5.600E-02	
Ba-133	80.99		6.171E-02		6.167E-02		6.190E-02	
Eu-152	121.78	6.676E-02	6.611E-02	-0.978%	6.623E-02	-0.796%	6.592E-02	-1.257%
Eu-152	244.69	5.599E-02	5.560E-02	-0.702%	5.561E-02	-0.691%	5.551E-02	-0.855%
Eu-152	344.28	4.720E-02	4.704E-02	-0.347%	4.742E-02	0.476%	4.712E-02	-0.178%
Cs-137	661.66		2.719E-02		2.700E-02		2.726E-02	
Eu-152	778.9	2.276E-02	2.300E-02	1.050%	2.286E-02	0.451%	2.310E-02	1.508%
Eu-152	964.13	1.798E-02	1.817E-02	1.019%	1.815E-02	0.931%	1.813E-02	0.833%
Co-60	1173.23		1.479E-02		1.476E-02		1.534E-02	
Co-60	1332.5		1.322E-02		1.330E-02		1.350E-02	
Eu-152	1408.01	1.248E-02	1.271E-02	1.869%	1.271E-02	1.877%	1.272E-02	1.947%
Nuclide	Energy	V2D2	P4V2D2		P5 V2D2		P6 V2D2	
			ETTM	Δ%	ETTM	Δ%	ETTM	Δ%
Am-241	59.53		4.785E-02		4.781E-02		4.765E-02	
Ba-133	80.99		5.279E-02		5.276E-02		5.296E-02	
Eu-152	121.78	5.745E-02	5.690E-02	-0.962%	5.700E-02	-0.781%	5.674E-02	-1.242%
Eu-152	244.69	4.782E-02	4.839E-02	1.191%	4.839E-02	1.202%	4.831E-02	1.034%
Eu-152	344.28	4.009E-02	4.117E-02	2.690%	4.151E-02	3.538%	4.124E-02	2.864%
Cs-137	661.66		2.405E-02		2.388E-02		2.411E-02	
Eu-152	778.9	1.973E-02	2.039E-02	3.322%	2.027E-02	2.710%	2.048E-02	3.790%
Eu-152	964.13	1.555E-02	1.616E-02	3.885%	1.614E-02	3.794%	1.613E-02	3.693%
Co-60	1173.23		1.319E-02		1.316E-02		1.368E-02	
Co-60	1332.5		1.181E-02		1.188E-02		1.206E-02	
Eu-152	1408.01	1.083E-02	1.136E-02	4.964%	1.136E-02	4.973%	1.137E-02	5.045%
Nuclide	Energy	V3D2	P4V3D2		P5 V3D2		P6 V3D2	
			ETTM	Δ%	ETTM	Δ%	ETTM	Δ%
Am-241	59.53		4.012E-02		4.008E-02		3.995E-02	
Ba-133	80.99		4.443E-02		4.440E-02		4.457E-02	
Eu-152	121.78	4.880E-02	4.808E-02	-1.464%	4.817E-02	-1.284%	4.795E-02	-1.743%
Eu-152	244.69	4.075E-02	4.120E-02	1.121%	4.121E-02	1.132%	4.114E-02	0.965%
Eu-152	344.28	3.442E-02	3.520E-02	2.271%	3.549E-02	3.116%	3.526E-02	2.445%
Cs-137	661.66		2.071E-02		2.056E-02		2.076E-02	
Eu-152	778.9	1.686E-02	1.759E-02	4.317%	1.748E-02	3.700%	1.767E-02	4.790%
Eu-152	964.13	1.359E-02	1.397E-02	2.760%	1.395E-02	2.670%	1.394E-02	2.570%
Co-60	1173.23		1.142E-02		1.140E-02		1.185E-02	
Co-60	1332.5		1.024E-02		1.030E-02		1.046E-02	
Eu-152	1408.01	9.465E-03	9.860E-03	4.170%	9.860E-03	4.179%	9.867E-03	4.250%

calibration for different position geometries. Where the values of the efficiency calculations using (ETTM) was compared with the measured ones as presented in table (5).

5. Conclusions

This work led to a simple (ETTM) to evaluate the FEPE over a wide energy range, which deal with different detector types for isotropic axial point sources, and axial cylindrical sources. Accordingly the present approach shows great possibilities to calibrate the detectors through the determination of the FEPE curve even in those cases when no standard source is available, which is considered as the final goal of this work. The discrepancies in general for all the measurements were found to be less (7%) between (ETTM) and experimental values at all energy region.

18.03.2013

Bibliography:

1. Le`py M.C., Altzitzoglou, T., Arnold, D., etal., 2001. Intercomparison of efficiency transfer software for gamma-ray spectrometry. Appl. Radiat. Isot. 55(4), 493–503.
2. Vidmar T., Aubineau Laniece, I., Anagnostakis, M.J., et al., 2008. An intercomparison of Monte Carlo codes used in gamma-ray spectrometry. Appl. Radiat. Isot. 66 (6–7), 764–768.
3. Abbas M.I. Appl. Radiat. Isot. 54 (2001), 761.
4. Abbas M.I. and Selim Y.S. Nucl. Instrum. Methods Phys. Res. A, 480/2-3 (2002) 649.
5. Abbas M.I., Nafee S.S. and Selim Y. S. Radiation Physics and Chemistry. 75 (2006) 729.
6. Abbas M.I. Journal of Physics D: Applied Physics 39 (2006) 3952.
7. Pibida L., Nafee S.S., Unterweger M., Hammond M.M., Karam L. and Abbas M. I. Applied Radiation and Isotopes Journal, 65 (2007) 225.
8. Abbas M.I. Nucl. Instrum. Methods Phys. Res. B, 256 (2007) 554.
9. Abbas M.I. Nuclear Technology 168 (2009) 41.
10. Abbas M.I. Nucl. Instrum. Methods Phys. Res. A, 615 (2010) 48.
11. Nafee S.S., Badawi M.S., Abdel-Moneim A.M., Mahmoud S.A. "Calibration of the 4p r-ray spectrometer using a new numerical simulation approach" Applied Radiation and Isotopes 68 (2010) 1746–1753
12. Debertin K. and Schotzig, U. 1979. Coincidence summing corrections in Ge(Li)-spectrometry at low source-to-detector distances, Nucl. Instrum. Meth. A158, 471.

M. S. Badawi, Physics Department, Faculty of Science, Alexandria University, 21511 Alexandria, Egypt. [Doctor], e-mail: ms241178@hotmail.com, Tel:+201005154976.
A. M. El-Khatib, Physics Department, Faculty of Science, Alexandria University, 21511 Alexandria, Egypt. [Professor. Doctor], e-mail: Elkhatib60@yahoo.com, Tel:+201000230122.
M. A. Elzaher, Department of Basic and Applied Sciences, Faculty of Engineering, Arab Academy for Science, Technology and Maritime Transport, Alexandria, Egypt. [Doctor], e-mail: mzaherdo@yahoo.com, Tel:+201141108373.
A. A. Thabet, Department of Medical Equipment Technology, Pharos University in Alexandria, Egypt. [Assistance Lecturer], e-mail: t.abuzeid@yahoo.com, Tel:+201111016886.
A. A. Sakr, Physics Department, Faculty of Science, Damanhour University, Egypt. [Doctor], e-mail: sakr22@yahoo.com, Tel:+201067012400.